Exploring the potential of waste leaf sheath date palm fibres for composite reinforcement through a structural and mechanical analysis

Alain Bourmaud[1], Hom Dhakal[2], Anouck Habrant[3], Justine Padovani[3],

David Siniscalco[1], Michael H. Ramage[4], Johnny Beaugrand[3,5], Darshil U. Shah[4]

[1]Université de Bretagne Sud, IRDL, FRE CNRS 3744, Lorient, France
[2]School of Engineering, University of Portsmouth, Portsmouth, Hampshire PO1 3DJ, United Kingdom
[3]Fractionnement des Agro Ressources et Environnement (FARE), INRA, University of Reims Champagne-Ardenne, 2 esplanade Roland Garros, F-51100 Reims, France
[4]Centre for Natural Material Innovation, Dept. of Architecture, University of Cambridge, Cambridge CB2 1PX, UK
[5]Biopolymères Interactions Assemblages (BIA), INRA, rue de la Géraudière, F-44316 Nantes, France

*Corresponding author: alain.bourmaud@univ-ubs.fr ; Phone: (+33) 297 874 518

Abstract

This work proposes a multi-scale study of the properties of leaf sheath date palm fibres currently considered as agricultural waste. Firstly, by using optical and electronic microscopy, two main types of bundles were identified which have profoundly different structures. Biochemical analysis and X-ray diffraction (XRD) revealed a low degree of crystallinity but a significant lignin content of about 17% giving the bundles a very cohesive structure as well as a good thermal stability in addition to a singular behaviour in dynamic vapour sorption. An average cell wall stiffness in the order of 16 GPa was highlighted by Atomic Force Microscopy in mechanical mode but tensile tests on bundles have revealed low stiffness and strength but a high elongation. These results combined with the cellular structure of these bundles, provides the potential of these wastes as cost effective and environmentally friendly composite reinforcements for high energy absorption and improved acoustics functions.

Keywords: Natural fibres; Chemical analysis; Microstructural analysis; Mechanical properties

1. Introduction

Over the past two decades, the use of plant fibres as reinforcements in composite materials has rapidly increased. These fibres have attracted major industrial interest because of their low price, competent specific mechanical performance [1,2], as well as potentially low environmental impact, lower than ubiquitous glass fibre reinforcements [3,4], especially if the former are secondary fibres (i.e. fibres are by-products from some other primary utilisation of the plants).

Plant fibres are derived from plant cell walls and therefore can have different origins within the plants. Some of them are found in the xylem of the plant, for example, fibres derived from wood [5]. Others are derived from the seeds, as in the case with cotton [6] and kapok [7]; these seminal hairs are not 'fibres' in the botanical sense of the term, but trichomes possessing a very specific structure and architecture. Due to their high microfibrillar angles and their very thin walls (for the kapok), they exhibit generally low mechanical properties. The other plant fibres are generally derived from the phloem of dicotyledonous plants or from tissues located at the periphery of the vascular bundles [8]. Among the phloem fibres, primary and secondary fibers are distinguished; primary fibres extracted from the cambium have the best properties because they have a structural role within the plant [9]. These plant include but are not limited to nettle [10], flax [11], hemp [12], and jute [13]. The fibres of the vascular tissues can be located in the culms (bamboo) [14], in the leaves of the monocotyledons (sisal or abaca) [15], in the mesocarp of the fruit (coir) [16] or around the trunks (palm trees) [17].

Date palm is cultivated extensively in North Africa and the Middle East, especially in Egypt, Iran and Saudi Arabia. In 2014, the global harvest area for date palm trees spanned 1.1 million hectares, with total collection of the high-value date fruit exceeding 7.6 million tonnes [18]. Date palm trees bear fruit 4-8 years after planting, and require a further 7-12 years to produce commercially viable yields [19,20]. Each year, the tree is pruned, including trimming of around 10-30 new leaves [20], leading to substantial waste generation: up to 35 kg biomass per tree, with the dry leaves accounting for as much as 20 kg [21–23]. Consequently, the accumulated bio-waste is non-trivial, in the order of millions of tonnes per annum. While there are a number of traditional uses of this bio-waste [19,20], a large amount of the residue is burnt or land-filled [21]. Currently, the fibres from the leaf sheaths are utilised for ropes and baskets, but also for the reinforcement of composite materials [24].

The palm tree stem is covered with a mesh made of fibre bundles, called fibrillum, creating a natural, woven mat of crossed fibres of different diameters. The fibrillum forms from the natural decomposition of leaf sheaths, and surrounds the remaining petioles of the old leaves. This fibrillum has a function of thermal protection of the plant [25] with entrapped air between the fibre bundles. It is currently considered as silviculture waste, and could constitute a form of supplementary income for the farmers. More efficient utilisation of this natural resource would also

have a positive impact on the environment. Their possible use for composite reinforcement may open a new market, for what are normally considered waste fibres, for use in low-value products.

Few studies are dedicated to the use of date palm fibres extracted from the tree. Alsaeed and Yousif [17] studied these fibres with an objective of using these fibres for composite reinforcement. They observed that the tensile strength between 100 and 400 MPa upon NaOH treatment of the fibres; a link between fibre critical length and diameter or NaOH treatment was highlighted. Alawar et al. [24] compared properties of date palm stem fibres before and after NaOH treatment. They found a tensile modulus and strength of 0.85 GPa and 245 MPa for raw fibres, respectively. A significant decrease in strength was measured after NaOH treatment, whereas Young's modulus increased. They hypothesise that a modification in the main cell-wall polysaccharides leads to the observed changes. An extensive piece of work carried out by AL-Oqla and Sapuan [26] on the feasibility of date palm fibre for light weight applications in the automotive industry suggests that natural fibres can be good candidate materials for composite reinforcement. They highlighted that date palm fibres can be used as sustainable materials for automotive applications. In the light of government regulations and consumer awareness, Yusoff et al. [27] analysed the mechanical properties of oil palm fibres. The oil plam/epoxy composites were fabricated at different fibre volume fractions. They pointed out that oil palm fibre can provide an effective reinforcing mecahnism to make light weight composites. Leman et al. [28] investigated the effect of environmental treatments on the fibre surface properties and its overall effects on the tensile properties of sugar palm fibre-reinforced epoxy composites. They suggested that seawater and freshwater treatments improved the surface properties of the sugar palm fibre, as well as their tensile properties through enhanced fibre matrix adhesion.

In this work, we examine fibres from the stems of the date palm tree (*Phoenix dactylifera*) especially fibres extracted from the leaf sheath with the intention of assessing their potential as reinforcements of composite materials. Precisely, the present work is aimed at evaluating the possibility of using date palm fibres derived from the tree stem (leaf sheath) as composite reinforcements. The results are presented in two phases with subtitles: phase (I) fibre properties and phase (II) composite properties. The second phase of this paper focuses on the investigation of the mechanical properties of date palm fibre reinforced composites, whereas this present paper, phase I, carries out a detailed analysis of the fibre in relation to its potential valorisation in composites. Firstly, an ultra-structural analysis of the bundles was conducted using light and scanning electron microscopy. Thereafter, a biochemical analysis was performed to quantify important cell-wall polysaccharide components (such as cellulose and lignin), as well as their structure (vis. cellulose crystallinity and microfibril angle using X-ray diffraction). The results obtained from the biochemical analysis were used to explain measured moisture sorption and mechanical behaviour of the fibres. Specifically, fibre mechanical properties were measured at both cell-wall and the fibre bundle scales by means of nanoindentation and fibre tensile testing, respectively.

2. Materials and methods

2.1. Materials

Raw samples of the mesh (natural mat) surrounding the date palm tree stems were brought from Al-Ahsa, located in the Eastern Province of Saudi Arabia. Bundle diameters were optically measured on around 100 samples, ranging between 100 and 800 µm. Density measurements, performed according to the previously described method [29], gave a value of 0.968 ± 0.002 g/cm^{-3}.

2.2. Microscopic observations

2.2.1. Optical microscopy

Two bundles of palm fibre, one millimetre in width and one much smaller were selected from the raw material and then cut transversely by hand. These samples were then embedded in polyethylene glycol (PEG) at progressively increasing concentration steps (30, 50 and 100%) at room temperature. The final embedding step was achieved in pure PEG at 70°C. 100 µm thick sections were obtained using a HM360 microtome, equipped with disposable microtome blades (Microm Microtech, France), and mounted on microscope slides. Some of the 100 µm thick sections were stained with a Congo Red solution, for which the PEG was removed prior to cyto-chemical staining by a washing step using deionized water. The Congo Red staining was done by 5 minutes immersion in the solution followed by a thorough washing step; in the process the (1,4)-β-glucan polymers (i.e. cellulose) and other polysaccharides(i.e. hemicellulose) are stained in red.

All observations were done using an Axioskop microscope equipped with an Axiocam MRc, at different magnification levels. Non-stained palm fibre sections were observed under visible (bright light) or UV (mercury lamp) light mode. Under UV light, we observed the blue fluorescence of phenolic (i.e. hydroxycinnamate and lignin) compounds upon excitation at 340 nm [30]. The Congo Red stained sections were observed under visible light.

2.2.1. SEM

Palm fibres were fractured by hand after immersion in liquid nitrogen. Scanning electron microscopy (SEM) images of the fracture surfaces were taken using a SEM Jeol JSM 6460LV. The samples were sputter-coated with a thin layer of gold in an Edwards Sputter Coater.

2.3. Biochemical investigations

2.3.1. Carbohydrate analysis

The identification and quantification of neutral and acid carbohydrates was carried out using high-performance anion-exchange chromatography (HPAEC) in the manner described previously [31], with a slight modification. To ensure representability, approximately 10 g of the palm fibre material was cryo-ground prior to hydrolysis. 2-deoxy-D-ribose was used as an internal standard and the

amount of neutral carbohydrates (arabinose, glucose, xylose, galactose, and mannose) were determined. In addition the acidic carbohydrates, galacturonic and glucuronic acids, were determined. The total carbohydrate content is the sum of the amounts of all monosaccharides and is expressed as a percentage of the dry palm fibers. Cellulose content was assumed on the basis of glucose monosaccharide content.

2.3.2. Lignin and ash content analysis

Lignin content was determined on three replicates using cryo-ground palm fibre using the Klason method described in [29]. The method is based on the quantification of the non-hydrolysable acid residue remaining after sulfuric acid hydrolysis. The ash content was subsequently determined after 4 h at 500°C.

2.4. X-Ray Diffraction

Wide-angle X-ray diffraction (WAXD) measurements were performed under ambient conditions on a Siemens D500 diffractometer CuKα radiation. Scans were collected from 2θ = 5 to 60° with step size of 0.03° at 4 s/step (Fig. 1). The beam was directed perpendicular to the fibre bundle length.

Crystallinity was calculated using Eq. 1, where I_{tot} is the intensity at the primary peak for cellulose I (at 2θ = 22.5°) and I_{am} is the intensity from the amorphous portion evaluated as the minimum intensity (at 2θ = 19.0°) between the primary and the secondary peaks (Fig. 1).

$$C = \frac{I_{tot} - I_{am}}{I_{tot}} \times 100 \qquad \text{(Eq. 1)}$$

Cellulose microfibril angle (MFA) in the S2 secondary cell wall layer was also estimated using the spectra. First, the T parameter was determined by Cave's [32] method using the primary peak for cellulose I. Thereafter, a polynomial equation proposed by Yamamoto et al. [33] was used to estimate MFA from the measured T-value.

2.5. Thermo-gravimetric analysis

Thermogravimetric analysis (TGA) was conducted using a Perkin Elmer Pyris 1 TGA. Palm fibre samples were scanned from ambient temperature to 800 °C at a heating rate of 10 °C/min under a 20 mL/min nitrogen gas flow (i.e. inert conditions).

2.6. Water absorption tests

Isotherms of water vapour desorption/sorption measurements were carried out using a Dynamic Vapour Sorption (DVS) instrument from Hiden Isochema Ltd. (UK). The procedure is similar to the one described in Guicheret-Retel [34]. In this study, the quantity used for both replicates was approx. 5 mg and the sequence of water sorption (10–90% relative humidity (RH) at 10% intervals) and desorption (90–15% RH at 15% intervals) was programmed.

Figure 1. XRD spectra of date palm tree stem fibres. Error bars indicate 1 std. dev.

2.7. Mechanical characterisation

2.7.1. Tensile test on palm fibre bundles

During selection of palm fibre bundles for testing, two broad groups of bundle types were observed: 'large' bundles with width on the mm scale and 'small' bundles, 3 to 5 times smaller than the former (discussed further in Section 3.1). Fibre bundles were randomly selected for the test; bundle width was not observed to have a noticeable effect on the measured mean strength properties.

The bundles' ends were encapsulated in resin to enable fibre gripping. These samples were prepared in sandwich plastic tabs (Diastron Ltd., Hampshire, UK), using a photo-curing glue and a UV-source pen. The samples have a gauge length of 10 mm.

Prior to testing, the samples were stored for 48h in a climatic chamber regulated at 20°C and 55% relative humidity. The cross-sectional areas of the samples was assessed with a dedicated and calibrated Fibre Dimensional Analysis System (FDAS, Diastron Ltd., Hampshire, UK), using a protocol similar to the one described in [35]. In this study, the samples were rotated within a laser beam with the full rotation scan mode (Fig. 2), on 5 equidistant slices along the palm fibre sample. The UvWin 3.40 Software gives the mean cross-section.

After dimensional assessment, the samples were tensile tested using a TEST108 2kN universal testing machine (GT-TEST, France), equipped with pneumatic side action grips (1kN, Instron) and the Testwinner software (Testwell®) in a climatic chamber (20°C; 55% RH). The displacement rate was set at 10 mm/min and the test was considered successful when failure occurred in the gauge length; 33 samples satisfied this criterion.

2.7.2. Nanoindentation and AFM Peak Force QNM measurements

Palm leave sheath bundles were embedded in a resin in order to maintain the fibre and the cell wall structure during sample surface preparation. Final resin polymerisation is done in an oven (60 °C, overnight). Then, the whole resin block with the sample is machined to reduce its cross section and an ultramicrotome (Leica Ultracut R) is then used with diamond knives (Diatom Histo and/or Ultra AFM) to cut a series of very thin sections (about 50 nm thick in the last step) at reduced cutting speed (≈1 mm/s) to minimise compression and sample deformation during the cutting process. This process allows us to decrease the surface roughness.

Figure 2. Fibre cross-section shape (bold black line) and area (shaded region) was estimated using a Fibre Dimensional Analysis System (FDAS). The coloured lines show the lines of path of laser beams that were tangential to a fibre surface.

A commercial nanoindentation system (Nanoindenter XP, MTS Nano Instruments) was used at room temperature (23 ± 1°C) with a continuous stiffness measurement (CSM) technique, equipped with a three-side pyramid (Berkovich) indenter. The system was operated at 3-nm amplitude, 45 Hz oscillations using a 0.05 s^{-1} loading rate. Measurements were taken at depths to 120 nm. Around 20 indents were performed in each sample.

In addition, mechanical characterization was performed by using a Multimode AFM (Bruker Corporation, USA). PF-QNM is an extension of the peak force Tapping™ mode where the vertical motion of the cantilever oscillates far below its resonant frequency (2 kHz). Each tapping event is an action of the probe indenting into the surface of the sample (typically 1-3 nm). RTESPA-525 (Bruker) probe was used. Its spring constant, around 200 N/m, was calibrated using the so-called Sader method [36] with a Scanning Electron Microscope (Jeol JSM 6460LV) for the measurements of the cantilever length and width, and the AFM in Tapping™ mode, for the measurement of its frequency response (resonance frequency and quality factor). The tip radius, between 9 nm and 50 nm, was tuned during a measurement on a Highly Oriented Pyrolytic Graphite (HOPG) standard from Bruker in order to obtain the indentation modulus of around 18 GPa, taking the adhesion force into account with a DMT contact model [37]. The applied maximum load (peak force) is set to 200 nN for all the measurements, leading to a contact stiffness of the same order as the cantilever stiffness for the studied materials [38]. The calibration was checked by comparing values obtained with those of nanoindentation.

3. Results and discussion

3.1. Focus on palm fibre structure

Figure 3 presents a schematic view of a date palm tree and the origin of the studied fibre bundles. Thanks to optical microscopy and SEM analysis, two main types of palm leaf sheath fibre bundles were identified in the collected fibrillum. Large bundles had an average diameter between 600 and 1000 μm, whereas the small bundles are around 70-120 μm. Figure 4 presents various views, obtained through optical microscopy, and highlighting the main morphological differences between the two fibre elements. Palm fibre bundle sections in (a)–(f) were examined by visible light microscopy, whereas (g)–(h) micrographs were observed under UV exposure. Histological features of non-stained small and large bundles are shown in (a) and (b), respectively. Congo red stained images (c) and (d) show a small and a large bundle, respectively, while (e) and (f) are focus of a large bundle. Firstly, one can notice the structural differences between the two kinds of bundles. The small ones exhibit a homogenous structure constituted of an assembly of elementary fibres with thick cell walls; single fibre diameter is approximatively 10 μm and cell wall thickness around 3-4 μm. Due to this specific organisation, these bundles have probably a mechanical role. Furthermore, the Congo red stained image (Fig. 4.c) is evidence of the presence of hemicellulose components within the cell walls, confirming a possible mechanical function of these fibre

elements and potential mechanical interest for composite applications. The UV induced auto fluorescence of fibre cell wall phenol components, highlighting preferentially lignified regions. One can notice blue fluorescence preferentially located in the middle lamella area; this phenomenon is usual on plant fibre such as flax [39]; lignin having a protection rule, enabling a strong bundle cohesion.

Interestingly, the large bundles have an opposite organisation and structure with thin cell walls (Fig. 4.f) and large lumens. One can also notice the presence of large vascular tissues with a diameter ~100-200 μm. The main function of these large bundles is to provide a conductive path in the leaf; the large vascular vessels probably enable to conduct the raw sap and the small bundles the elaborated one. Congo red stanining experiments reveal low hemicelluloses or cellulose content in the cell walls except in the vascular vessels area, these localised and specific structures can be developed in order reinforce the stiffness in the vascular areas to protect these essential elements. Bundles stiffness can also be ensured by high lignification rate of the cell walls, compared to the small bundles, as highlighted on Fig 4.h. Another explanation of this reaction to Congo red can be the age of the cell walls; the younger ones may possibly be less lignified.

These two bundles are made of mostly cellulose, hemicelluloses and lignin arranged in a highly ordered but different structure. Consequently, the mechanical performances of the two kind of bundles can differ but their specific ultrastructure can be complementary. Due to their specific honeycomb structure we can suppose that the large bundles have probably interesting energy absorption impact properties; these points will be deeply investigated in mechanical section of this paper but also on a forthcoming paper, dedicated to composite reinforcement.

Figure 3. Schematic view of fibre bundles origin and identification.

Figure 4. Optical microscope observations, scale bars are 100μm in all the micrographs.

A final analysis in this descriptive section focusses on the presence of silica, which was noticed through SEM analysis (Fig. 5). In our case, silica is found embedded in the surface of large bundles (Fig.5). According to Esau [40] silica can be deposited in monocotyledonous cell walls and especially in leaves where content can be as high as 41%-wt. In palm, small silica cells are formed and called stegmata [41]. The presence of silica causes many kinds of problems in pulping and papermaking. Silica accumulation in plants contributes to the strength of stems and provides resistance to attack by pathogenic fungi and predaceous chewing insects and other herbivores [42]. With lignin, the production of stegmata by the rind provides additional mechanical defence for the plant. Finally, the presence and the shape of the silica bodies can be an interesting way for species identifications as underlined by Prychid et al. [43]. Fibre surface defects, such as silica bodies may affect overall composites properties. The defects can act as stress concentrators and damage can initiate from such defects. We observed clear defects on the fibre element structures,

with the pits with silicate bodies arguably providing crack departure mechanisms or being surface flaws in view of composite properties.

3.2. Biochemical and XRD analysis

Table 1 shows chemical composition of the date palm leaf sheath fibres bundles. Additional values are indicated about literature data on both palm element and other plant fibres. Firstly, one can notice an interesting cellulose rate (45.1±3.4%); this cellulose content is well correlated with value of Saadoui et al. [44] on palm fibrillum and is in the same range than bamboo or coir fibres. Our samples are characterized by an important lignin content, especially compared to phloem bast fibres such as hemp or flax; indeed, these plants are harvested between the lignification process in order to facilitate the retting and the mechanical extraction; in vascular cambium tissues, i.e. palm, bamboo, sisal or coir, lignin is preponderant for the plant and contribute to its protection against exogenous attacks (water, insects…) by reinforcing the bundle stiffness.

Figure 5. SEM observations of silica bodies.

Table 1. Chemical composition (dry wt%; mean ± st. dev.) of the date palm tree fibres.

Hemicelluloses content is also high but this value must be treated with caution; indeed, our synthesis hemicelluloses, for a homogenous comparison with literature date, represents the whole cell wall polysaccharides whatever their chain length and their linkage or reinforcement capacity. According to the biochemical method, the precise quantification of matrix or structuring polysaccharides is not possible. Several authors [48–50] showed that according to their structure, pectins components can highly impact the stiffness and mechanical performances of flax fibres. The strong contribution of galactans into cell wall stiffness was also proved [51] as well as their main rule into the structuration of gelatinous cell walls (G-layer).

In agreement with Van Dam and Gorshkova [8] or Chernova and Gorshkova [52], plant fibres can be classified into two broad categories from a biochemical and structural point of view. The first consists of xylan-type cell walls and is the most widespread, it involves different types of wooden cells, but it is also found in fibers derived from stems such as jute or kenaf. These walls are characterized by a high microfibrillar angle (MFA), by small thicknesses of secondary walls (generally between 1 and 4 µm), but also by high levels of lignin and xylan. The G-layer form the second group; They have the particularity of possessing matrix polymers rich in galactose and high cellulose contents of up to 85%. Unlike xylan fibres, these cell walls exhibit very small MFA as well as high wall thicknesses, generally between 10 and 15 µm. These fibres are mainly derived from the phloem of flax, hemp or even ramie but can also be found in bamboo. To better understand the specific composition of our fibres, carbohydrate analysis is detailed in the first line of Table 1. Due to their high xylose and lignin content, palm leave sheath fibres are part of the

xylan group; this assumption is also confirmed by their low galactose content, especially by comparison with bast fibres such as hemp [53].

To complete the biochemical analysis, we measured the crystallinity of the date palm fibres using XRD to be 41 ± 3 %, comparable to literature (Table 2). Both, the measured cellulose content and crystallinity of the date palm fibres are at the lower end of other leaf fibres (Table 2), such as banana (70-82wt%, 44-60%) and pineapple (44-64wt%, 45-55%), but higher than that of seed fibres such as coir (32-43wt%, 27-33%) and fibres from oil palm empty fruit bunch (40-50wt%, 20-30%) [47]. The measured MFA of the date palm fibres was 26.1 ± 14.2°, which is also in agreement with literature (Table 2), and intermediate to leaf and seed fibres. As is discussed later, the tensile properties of date palm leaf fibres also exhibit this inclination.
In general, whether by biochemical or microstructural analysis, important results such as hemicellulose and lignin content, MFA and presence of silica bodies were highlighted. When considering these fibres as composite reinforcement, this information needs to be taken into account; the link between plant fibre structure and fibre or composite properties has been demonstrated by many authors [54,55].

3.3. Thermo-gravimetric analysis

The thermal degradation behaviour of the date palm fibres was examined through TGA and compared with other natural fibres (Fig. 6). Initial mass loss of 6.0 wt% up to 200 °C was attributed to moisture evaporation. This is typical of natural fibres [56] albeit measured to by higher in our date palm fibres, similar to bamboo. Thereafter, the onset of thermal degradation and rapid mass loss was at 270 °C, with the maximum degradation rate occurring at 410 °C; both are much higher than other natural fibres. This point is particularly interesting for a future use of palm fibres as composite reinforcement; due to their important lignin content, their high degradation temperature can allow an association with a large range of thermoplastic polymers. These measurements are useful in determining the maximum processing temperature of the fibres during composite manufacture without substantial fibre degradation, and for example, selection of an appropriate thermoplastic. Notably, fibre mechanical property degradation may start earlier than the onset temperature for thermal degradation. Substantial degradation between 250 and 450°C was attributed to decomposition of the organic cell wall polysaccharides, with denaturation and charring occurring beyond 450 °C. Unlike other natural fibres, which typically show one degradation peak (in the range of 250 to 350 °C), the date palm fibres are unique in that they show two distinct degradation peaks: a primary peak at 410 °C, and a secondary peak in the typical in 250-350 °C region indicating better thermal stability compared to other commonly used natural fibres. Evidently, bamboo does show a minor secondary peak as well. The higher degradation temperatures of date palm fibres may be due to the higher observed silica content. A residual mass of 15.9 wt% was measured when heated to 800 °C, which would be a mixture of charred organic material and inorganic inclusions, such as the silica bodies.

3.4. Sorption behaviour

Moisture absorption and desorption isotherm plots for the date palm tree fibres are presented in Figure 7, with a comparison to other natural fibres. Classic sigmoidal-shaped (type II) isotherms were observed, as well as a hysteresis response, similar to that of other plant fibres [57,58].
The isotherm plots can be described by three regions [57]: i) Region A, up to 10% RH, where water is principally absorbed through hydrogen bonding by amorphous cellulose and hemicellulose in the inner-most cell wall layer, until saturation, ii) Region B, between 10 and 60% RH, where the porous structure of the fibres and cell wall enables absorption of water into the other cell wall layers through micro-capillaries, and iii) Region C, above 60% RH, where capillary condensation dominates and water molecules aggregate to form a fluidic, bulk phase.

Table 2. Comparison of mechanical and governing bio-chemical properties of our date palm tree stem fibres with various other plant fibres. Data from [47] and references therein.

Figure 6. Thermal degradation behaviour of date palm fibres in comparison to other natural fibres.

Figure 7. Moisture sorption behaviour of date palm tree stem fibres in comparison to other natural fibres. Data on other natural fibres from Hill et al [57].

The hysteresis response can be explained by the differing conditions in which sorption and desorption take place [57]. During adsorption, the date palm fibres deform by swelling and the micro-capillaries expand. However, during desorption, relaxation to the previous state is kinetically hindered, leading to a larger free volume (i.e. micro-capillary space) in comparison to the adsorption state.
Comparing to Hill et al's [57] data on various natural fibres (Fig. 7), the date palm fibres have very similar isotherm profiles to coir (coconut palm) and Sitka spruce wood, including the total moisture content at a given relative humidity (approaching 24% at 90% RH) and the high degree of hysteresis exhibited. In fact, hysteresis for the date palm fibres peaks to as much as 4% between 50-70% RH; this is substantially higher than the typically 1.5-3.2% peak hysteresis recorded for other plant fibres [57]. High amorphous polysaccharide content (amorphous cellulose, hemicellulose, and lignin) give the date palm fibres high water accessibility (through hydrogen bonding) leading to the high moisture uptake. The high degree of hysteresis may be explained by the high lignin content of the date palm fibres [57], and the presence of substantial micro-scale porosity in the fibre surface (filled with silica bodies; Fig. 5). However, most interestingly, the date palm fibres were also found to be unique, in that in comparison to the other fibres (including jute, coir, flax, hemp and cotton), they have the largest RH region (up to 10%), where adsorption and desorption curves overlap (i.e. 0% hysteresis region). This may give the date palm fibres a capacity to absorb and hold moisture, potentially of vital importance in supporting the growth of these date palm trees which generally grow in water-scarce regions.

3.5. Multi-scale mechanical properties of palm fibres

3.5.1. Bundles tensile characterization

At the fibre scale, tensile tests were carried out on fibre bundles. Prior to tensile testing, fibre cross-section properties were measured through a Fibre Dimensional Analysis System (FDAS). We found that the date palm fibre bundles were often better approximated by elliptical cross-sections than circular cross-sections (Fig. 2). The elliptical geometry approximation, which is closer to the true cross-section shape, yielded areas 14 ± 7% larger than those obtained by circular geometry approximation based on a measured mean diameter/width. Notably, the irregular cross-section of plant fibres and insensitive (yet prevalent) area measurement approaches (e.g. 'apparent' area based on an assumed circular cross-section shape and measurement of mean diameter/width) have been a major source of error in many plant fibre testing studies [59]. A number of studies have shown that the true cross-section area can be up to 1.42 to 2.55 times lower than the apparent cross-section area [60–62], leading to an underestimation of fibre properties (strength and stiffness) by up 40-70%. Here, the use of an FDAS enables more accurate measurement of fibre geometrical properties, for use in mechanical property calculations.

The key fibre mechanical properties measured through the fibre bundle tensile tests are presented in Table 2. The Young's modulus, measured in the initial linear region, was obtained as 1.8 ± 0.6 GPa. A knee in the stress-strain curve, indicative of a yield point, was noticeable at *ca* 2% applied strain. Failure strength and strain of 131 ± 34 MPa and 20.9 ± 7.6% were measured. Fibre toughness, estimated by the area under the tensile stress-strain curve, was 13.9 ± 6.9 MJm^{-3}.

Table 2 and the Ashby charts in Fig. 8 and compare the mechanical properties of our date palm tree stem fibres with those of various other plant fibres. In terms of stiffness and strength, both absolute and specific, it is evident that the date palm tree stem fibres register the lowest properties. However, these properties are closer to that of seed fibres, such as cotton, oil palm and especially coir (coconut palm). The failure strains of these various palm fibres (date palm, oil palm and coir) are large and in a similar range (15-30%). The large failure strain results with a moderate toughness of the date palm fibre, comparable to strong-brittle bast fibres, like flax.

The primary structural polysaccharide in the plant fibre cell wall is cellulose, which exhibits both crystalline and amorphous regions. The mechanical properties of ordered, crystalline cellulose (both along and transverse to the chain direction) are substantially higher than that of amorphous cellulose, as well as the other amorphous polysaccharides (vis. hemicellulose and lignin) [63]. Furthermore, cellulose microfibrils are helically wound around the cell walls, and therefore are at an angle with respect to the fibre axis. Consequently, biochemical properties, particularly cellulose content, cellulose crystallinity, and MFA are well-known to have a profound effect on fibre mechanical properties [47,64].

Table 2 compares the mechanical and the relevant biochemical properties of the date palm tree stem fibres with other plant fibres. It is obvious that bast fibres, with the highest stiffness and strength, and low failure strains, have high cellulose content (60-75%), high cellulose crystallinity

(up to 90%) and the cellulose microfibrils are closely aligned to the fibre axis (MFA <10°). Leaf fibres with moderate stiffness, strength and failure strains have slightly high cellulose content (up to 80%), moderate cellulose crystallinity (up to 70%) and higher MFA (up to 25°). Finally, seed fibres with the lowest stiffness and strength, but high ductility, have low cellulose content (typically less than 50%), cellulose crystallinity (up to 50%), and large MFA (30-50°). Indeed, the comparable mechanical properties of our date palm fibres with the seed fibres, particularly other palm fibres (oil, coconut) can be explained by their comparable biochemical properties. Moreover, palm bundles exhibit a specific structure with single cells having important lumens which is not in favour of high longitudinal tensile performances. These objects can be more interesting for energy absorption thanks to their structure and high elongation at break. This point will be explored in the second paper dedicated to the use of palm fibers for composite reinforcement.

Figure 8. Materials Ashby chart of absolute (a) and specific (b) tensile stiffness and strength. Adapted from [2].

While the tensile modulus and strength of the date palm fibres is observed to be very low, this however, is not a deterrent for use in composites applications. Firstly, as the fibres are bio-waste, their utilisation, even as fillers, replacing a sizeable fraction of the more environmentally-polluting matrix, can lead to sustainable materials, particularly if the matrix is a thermoplastic or biodegradable. Secondly, the date palm fibres have properties not very different to seed fibres, like cotton, and cotton fibre composites are by far the most widely used non-wood plant fibres in biocomposites applications for the automotive industry: 100,000 tonnes cotton fibre composites were produced in the EU in 2010, in comparison to 45,000 tonnes of non-wood, non-cotton plant fibre composites [47].

3.5.2. Nanoindentation and Peak Force-QNM measurements

Table 3 shows nanoindentation modulus and hardness values obtained on both large and small bundles. Regarding the nanoindentation modulus, palm stiffness values are in the same range that jute, sisal or hemp fibres studied in a previous study [65]

On mature plant cell walls, the longitudinal nanoindentation modulus is generally included between 15 and 22 GPa [66–69] and differences are often low between various plant fibres. Indeed, whatever on wood of plant cell walls this value is low compared to the modulus obtained by with conventional tensile tests [68,70]. The variations between varieties could be induced by variations in the microfibrillar angle (MFA) of the crystalline cellulose or by the cellulose:matrix volume ratio as evidenced by Tze et al. [71]. In this way and as assumed by Konnerth et al. [66,70] and Gindl et al. [70], the hardness behaviour is dominated by polymers constituting the polysaccharide cell matrix, i.e. hemicelluloses, lignin and pectins. The nanoindentation modulus is more linked to the cellulose properties and to their microfibrillar angle. The indentation hardness is generally included

between 0.25 and 0.45 GPa for wood [67,72] or flax cell walls [68,73]; thus, the monitoring of this parameter is an interesting way to estimate variations or scattering into the polysaccharidic matrix. In our case, one can notice that palm cell walls nanoindentation modulus is high and not well correlated with the tensile one regarding to literature data [65]. Nevertheless, it is not pertinent to compare palm bundles with bast fibres such as jute, flax or hemp. Morphologically speaking, these fibres are strongly different and even if cell wall stiffness is quite similar, their specific structure with fine cell walls and important lumen give them a different mechanical behaviour underlined by low stiffness and important elongation at break (Table 2). Regarding the cell wall hardness, interestingly, the important measured value indicate a hard polysaccharidic matrix; this point corroborates the biochemical conclusions and the important lignin content as compared to other plant fibres.

These nanoindentation data were supported by an AFM PF-QNM analysis at the cell wall scale. Indeed, nanoindentation provides a global cell wall stiffness information but the relative indent size compared to cell wall doesn't support to finely describe the cell wall mechanical properties. In this way, Figure 9 proposes PF-QNM stiffness mapping of small and large bundles cell walls.

Firstly, one can notice an interesting correlation between the two investigation ways. The S2 layers PF-QNM values are very close to those obtained with nanoindentation. Whether for small and large bundles, the cell walls stiffness are around 16 GPa; this PFQNM modulus value is in good agreement with values obtained by other AFM techniques for similar layers in wood or flax cell walls [38,74]. Interestingly, one can notice that the indentation modulus of the middle lamella (CML) area is around 10-12 GPa, this results is higher than nanoindentation results for flax [74] and can be explained by high lignin content in palm cell walls.

In addition, one can compare the morphological and mechanical structure of the two kinds of bundles. As expected and previously observed in Figure 4, large bundles exhibit cells having large lumens as compared to small bundles. Nevertheless, cell wall thickness are in the same range and around 1.5 μm. We can clearly observe the presence of different domains, S2 layer of the fibres are clearly visible as well as the middle lamellas linking the fibres together. On specific fibres, it is also possible to distinguish a thick S1 layer. One can notice the high middle lamella thickness leading probably to very cohesive bundles.

Table 3. Palm bundles nanoindentation properties.

Figure 9. PF-QNM modulus mapping obtained for large and small palm bundles. A profile of the stiffness is indicated under each image, corresponding to the black line.

In this section, PF-QNM and nanoindentation, experiments were combined to investigate the cell wall mechanical performances of palm bundles. Interestingly PF-QNM confirms nanoindentation values and gives pertinent information in terms of cell wall bundles structure and morphology.

4. Conclusions

In this work we studied the structure as well as the physio-chemical and mechanical properties of palm leaf sheath fibre bundles at different scales. We were able to identify two types of bundles, each with a specific function in the plant. Those with a larger diameter are conduction bundles made up of cells having thin walls and large lumens while the smaller ones with lumens of a much smaller size which are dedicated to a more structural function.

The biochemical analyses revealed a significant lignin and xylose content which makes it possible to classify these walls as the xylan type. Their high lignin content, highlighted in middle lamellas by PeakForce-QNM stiffness measurements gives them good thermal stability as well as an original sorption behaviour, with a wide hysteresis range which allows them to have good performances in terms of water absorption and storage.

On the other hand, their mechanical performances at the bundle scale are moderate in terms of stiffness and strength. This is not found at the cell wall scale. Thus, the nanoindentation and PeakForce-QNM showed rigidities of cell walls close to those of other fibers extracted from the plants. The bundle behaviour is compromised by the small cell wall thickness and the large relative lumen size. On the other hand, these bundles possess a high elongation at break. The combination of good deformation and of their cohesive structure can enable them to be integrated into composites with an energy absorption function. This point will be more deeply studied in another paper.

Acknowledgements

The authors thank Miguel Pernes, and Francois Gaudard from INRA for their technical assistance,. Dr Johnny Beaugrand is thankful for the support provided by the MATRICE state-to-country (Région Alsace Champagne-Ardenne Lorraine) program, France. Dr Darshil Shah and Dr Michael Ramage were supported by a Leverhulme Trust Grant. Dr Alain Bourmaud thanks Region Bretagne and OSEO for the FIABILIN programme funding.

References

[1] Baley C, Bourmaud A. Average tensile properties of French elementary flax fibers. Mater Lett 2014;122:159–61. doi:http://dx.doi.org/10.1016/j.matlet.2014.02.030.

[2] Shah DU. Natural fibre composites: Comprehensive Ashby-type materials selection charts. Mater Des 2014;62:21–31. doi:10.1016/j.matdes.2014.05.002.

[3] Shah DU, Schubel PJ, Clifford MJ. Can flax replace E-glass in structural composites? A small wind turbine blade case study. Compos Part B Eng 2013;52:172–81. doi:10.1016/j.compositesb.2013.04.027.

[4] Le Duigou A, Baley C. Coupled micromechanical analysis and life cycle assessment as an integrated tool for natural fibre composites development. J Clean Prod 2014;83:61–9. doi:http://dx.doi.org/10.1016/j.jclepro.2014.07.027.

[5] Ruelle J, Yoshida M, Clair B, Thibaut B. Peculiar tension wood structure in Laetia procera (Poepp.) Eichl. (Flacourtiaceae). Trees 2007;21:345–55. doi:10.1007/s00468-007-0128-0.

[6] Ansell MP, Mwaikambo LY. 2 – The structure of cotton and other plant fibres. Handb. Text. Fibre Struct., 2009, p. 62–94. doi:10.1533/9781845697310.1.62.

[7] Fengel D, Wenzkowski M. Studies on Kapok 1. Electron Microscopic Observations. Holzforshung 1986;40:137–41.

[8] van Dam JEG, Gorshkova TA. Encyclopedia of Applied Plant Sciences. Elsevier; 2003. doi:10.1016/B0-12-227050-9/00046-6.

[9] Bourmaud A, Gibaud M, Lefeuvre A, Morvan C, Baley C. Influence of the morphology characters of the stem on the lodging resistance of Marylin flax. Ind Crops Prod 2015;66:27–37. doi:10.1016/j.indcrop.2014.11.047.

[10] Bodros E, Baley C. Study of the tensile properties of stinging nettle fibres (Urtica dioica). Mater Lett 2008;62:2143–5.

[11] Gorshkova TA, Wyatt SE, Salnikov V V, Gibeaut DM, Ibragimov MR, Lozovaya V V, et al. Cell-wall polysaccharides of developing flax plants. Plant Physiol 1996;110:721–9.

[12] Crônier D, Monties B, Chabbert B. Structure and Chemical Composition of Bast Fibers Isolated from Developing Hemp Stem. J Agric Food Chem 2005;53:8279–89.

[13] Roy A, Chakraborty S, Kundu SP, Basak RK, Majumder SB, Adhikari B. Improvement in mechanical properties of jute fibres through mild alkali treatment as demonstrated by utilisation of the Weibull distribution model. Bioresour Technol 2012;107:222–8. doi:http://dx.doi.org/10.1016/j.biortech.2011.11.073.

[14] ABDUL KHALIL HPS, ALWANI MS, ISLAM MN, SUHAILY SS, Dungani R, H'ng YM, et al. The use of bamboo fibres as reinforcements in composites. In: Elsevier, editor. Biofiber Reinf. Compos. Mater. Woodhead P, London: 2015, p. 488–524. doi:10.1533/9781782421276.4.488.

[15] Silva F de A, Chawla N, Filho RD de T. Tensile behavior of high performance natural (sisal) fibers. Compos Sci Technol 2008;68:3438–43. doi:10.1016/j.compscitech.2008.10.001.

[16] Gu H. Tensile behaviours of the coir fibre and related composites after NaOH treatment. Mater Des 2009;30:3931–4.

[17] Alsaeed T, Yousif BF, Ku H. The potential of using date palm fibres as reinforcement for polymeric composites. Mater Des 2013;43:177–84. doi:10.1016/j.matdes.2012.06.061.

[18] Food and Agriculture Organization of the United Nations. FAOSTAT dataset 2017.

[19] Chao C., Krueger R. The Date Palm (Phoenix dactylifera L.): Overview of Biology, Uses, and Cultivation. Hortscience 2007;42:1077–82.

[20] Barreveld WH. Dates palm products. FAO Agric Serv 1993;101.

[21] Nasser RA, Salem MZM, Hiziroglu S, Al-Mefarrej H., Mohareb A., Alam A., et al. Chemical Analysis of Different Parts of Date Palm (Phoenix dactylifera L.) Using Ultimate, Proximate and Thermo-Gravimetric Techniques for Energy Production. Energies 2016;9:374. doi:10.3390/en9050374.

[22] Chandrasekaran M, Bahkali A. Valorization of date palm (Phoenix dactylifera) fruit processing by-products and wastes using bioprocess technology - Review. Saudi J Biol Sci 2013;20:105–20. doi:10.1016/j.sjbs.2012.12.004.

[23] El-Juhany LI. Surveying of Lignocellulosic Agricultural Residues in Some Major Cities of Saudi Arabia. vol. 1. Riyadh, Saudi Arabia: 2001.

[24] Alawar A, Hamed AM, Al-Kaabi K. Characterization of treated date palm tree fiber as composite reinforcement. Compos Part B Eng Nat Fiber Compos 2009;40:601–6. doi:10.1016/j.compositesb.2009.04.018.

[25] Oushabi, Sair A, YAbboud Y, Tanane O, Čigášová J. Natural thermal-insulation materials composed of renewable resources: characterization of local date palm fibers (LDPF). J Mater Environ Sci 2015;6:3395–402.

[26] AL-Oqla FM, Sapuan SM. Natural fiber reinforced polymer composites in industrial applications: feasibility of date palm fibers for sustainable automotive industry. J Clean Prod 2014;66:347–54. doi:10.1016/j.jclepro.2013.10.050.

[27] Yusoff MZ., Sapuan S., Ismail N, Wirawan R. Mechanical properties of oil palm fibre reinforced epoxy composites. Sains Malaysiana 2010;39:87–92.

[28] Leman Z, Sapuan S., Azwan M, Maleque M., Ahmad MMH. The effect of environmental treatments on fiber surface properties and Tensile strength of sugar palm fibre reinforced epoxy composites. Polym Plast Technol Eng 2008;47:606–12.

[29] Beaugrand J, Nottez M, Konnerth J, Bourmaud A. Multi-scale analysis of the structure and mechanical performance of woody hemp core and the dependence on the sampling location. Ind Crops Prod 2014;60. doi:10.1016/j.indcrop.2014.06.019.

[30] Beaugrand J, Paës G, Reis D, Takahashi M, Debeire P, O'Donohue M, et al. Probing the cell wall heterogeneity of micro-dissected wheat caryopsis using both active and inactive forms of a GH11 xylanase. Planta 2005;222:246–57. doi:10.1007/s00425-005-1538-0.

[31] Beaugrand J, Crônier D, Thiebeau P, Schreiber L, Debeire P, Chabbert B. Structure, Chemical Composition, and Xylanase Degradation of External Layers Isolated from Developing Wheat Grain. J Agric Food Chem 2004;52:7108–17. doi:10.1021/jf049529w.

[32] Cave ID. X-Ray Measurement of Microfibril Angle. For Prod J 1966;44:37 – 4.

[33] Yamamoto H, Okuyama T, Yoshida M. Method of Determining the Mean Microfibril Angle of Wood Over a Wide Range by the Improved Cave's Method. Mokuzai Aaagkkaish 1993;39:11–1.

[34] Guicheret-Retel V, Cisse O, Placet V, Beaugrand J, Pernes M, Boubakar ML. Creep behaviour of single hemp fibres. Part II: Influence of loading level, moisture content and moisture variation. J Mater Sci 2015;50:2061–72. doi:10.1007/s10853-014-8768-0.

[35] Haag K, Müssig J. Scatter in tensile properties of flax fibre bundles: influence of determination and calculation of the cross-sectional area. J Mater Sci 2016;51:7907–17. doi:10.1007/s10853-016-0052-z.

[36] Sader J., Sanelli J., Adamson B., Monty J., Wei X, Crawford S., et al. Spring constant calibration of atomic force microscope cantilevers of arbitrary shape. Rev Sci Instrum 2012;83:103705.

[37] Barthel E. Adhesive elastic contacts: JKR and more. J Phys D Appl Phys 2008;41:163001.

[38] Arnould O, Arinero R. Towards a better understanding of wood cell wall characterisation with contact resonance atomic force microscopy. Compos Part A-Appl Sci 2015;74:69–76.

[39] Gorshkova TA, Salnikov V V, Pogodina NM, Chemikosova SB, Yablokova E V, Ulanov A V, et al. Composition and Distribution of Cell Wall Phenolic Compounds in Flax (Linum usitatissimum L.) Stem Tissues. Ann Bot 2000;85:477–86.

[40] Esau K. Plant Anatomy. New York: Wiley; 1953.

[41] Jeyasingam J. Problems facing non wood pulp and paper mills due to the presence of silica: from raw material preparation to the finishing of paper 9-11. Nonwood plant fiber pulping, Atlanta: 1986, p. 9–11.

[42] McNaughton SJ, Tarrants J. Grass leaf silici- fication: Natural selection for an inducible defense against herbivores. Proc Natl Acad Sci 1983:790–791.

[43] Prychid CJ, Rudall PJ, Gregory M. Systematics and biology of silica bodies in monocotyledons. Bot Rev 2004;69:377–440.

[44] Saadaoui N, Rouilly A, Fares K, Rigal L. Characterization of date palm lignocellulosic by-products and self-bonded composite materials obtained thereof. Mater Des 2013;50:302–8. doi:10.1016/j.matdes.2013.03.011.

[45] Zhang T, Guo M, Cheng L, Li X. Investigations on the structure and properties of palm leaf sheath fiber. Cellulose 2015;22:1039–51. doi:10.1007/s10570-015-0570-x.

[46] Lewin M. Handbook of Fiber Chemistry, Third Edition. CRC Press; 2006.

[47] Shah DU. Developing plant fibre composites for structural applications by optimising composite parameters: a critical review. J Mater Sci 2013;48:6083–107. doi:10.1007/s10853-013-7458-7.

[48] Alix S, Goimard J, Morvan C, Baley C. Influence of pectin structure on mechanical properties of flax fibres: a comparison between a linseed-winter variety (Oliver) and a fibres-spring variety of flax (Hermès). Pectins and Pectinases 2009;in: H.A. S:87–96.

[49] Lefeuvre A, Duigou AL, Bourmaud A, Kervoelen A, Morvan C, Baley C. Analysis of the role of the main constitutive polysaccharides in the flax fibre mechanical behaviour. Ind Crops Prod 2015;76. doi:10.1016/j.indcrop.2015.07.062.

[50] Bourmaud A, Morvan C, Bouali A, Placet V, Perré P, Baley C. Relationships between micro-fibrillar angle, mechanical properties and biochemical composition of flax fibers. Ind Crops Prod 2013;44. doi:10.1016/j.indcrop.2012.11.031.

[51] Gorshkova T, Morvan C. Secondary cell-wall assembly in flax phloem fibres: Role of galactans. Planta 2006;223:149–58.

[52] Chernova TE, Gorshkova T. Biogenesis of plant fibers. Russ J Dev Biol 2007;38:221–32.

[53] Beaugrand J, Nottez M, Konnerth J, Bourmaud A. Multi-scale analysis of the structure and mechanical performance of woody hemp core and the dependence on the sampling location. Ind Crops Prod 2014;60:193–204. doi:10.1016/j.indcrop.2014.06.019.

[54] Coroller G, Lefeuvre A, Le Duigou A, Bourmaud A, Ausias G, Gaudry T, et al. Effect of flax fibres individualisation on tensile failure of flax/epoxy unidirectional composite. Compos Part A Appl Sci Manuf 2013;51:62–70. doi:http://dx.doi.org/10.1016/j.compositesa.2013.03.018.

[55] Summerscales J, Dissanayake NPJ, Virk AS, Hall W. A review of bast fibres and their composites. Part 1 – Fibres as reinforcements. Compos Part A Appl Sci Manuf 2010;41:1329–35. doi:10.1016/j.compositesa.2010.06.001.

[56] Leuwin M. Handbook of fiber chemistry. Boca Raton. 2007.

[57] Hill CAS, Norton A, Newman G. The Water Vapor Sorption Behavior of Natural Fibers. J Appl Polym Sci 2009;112:1524–1537. doi:10.1002/app.29725.

[58] Celino A, Freour S, Jacquemin F, Casari P. The hygroscopic behavior of plant fibers: a review. Front Chem 2014;1. doi:10.3389/fchem.2013.00043.

[59] Shah D, Nag N, Clifford M. Why do we observe significant differences between measured and “back-calculated” properties of natural fibres? Cellulose 2016. doi:10.1007/s10570-016-0926-x.

[60] Thomason JL, Carruthers J, Kelly J, Johnson G. Fibre cross-section determination and variability in sisal and flax and its effects on fibre performance characterisation. Compos Sci Technol 2011;71:1008–15. doi:10.1016/j.compscitech.2011.03.007.

[61] Virk A. Numerical models for natural fibre composites with stochastic properties. University of Plymouth, 2010.

[62] D’Almeida J, Mauricio M, Paciornik S. Evaluation of the cross-section of lignocellulosic fibers using digital microscopy and image analysis. J Compos Mater 2012;46:3057–65.

[63] Placet V, Trivaudey F, Cisse O, Gucheret-Retel V, Boubakar ML. Diameter dependence of the apparent tensile modulus of hemp fibres: A morphological, structural or ultrastructural effect? Compos Part A Appl Sci Manuf 2012;43:275–87. doi:10.1016/j.compositesa.2011.10.019.

[64] Pickering K. Properties and Performance of Natural-Fibre Composites. Elsevier; 2008.

[65] Tanguy M, Bourmaud A, Baley C. Plant cell walls to reinforce composite materials: Relationship between nanoindentation and tensile modulus. Mater Lett 2016;167. doi:10.1016/j.matlet.2015.12.167.

[66] Konnerth J, Gierlinger N, Keckes J, Gindl W. Actual versus apparent within cell wall variability of nanoindentation results from wood cell walls related to cellulose microfibril angle. J Mater Sci 2009;44:4399–406.

[67] Gindl W, Gupta H-S, Schöberl T, Lichtenegger H-C, Fratzl P. Mechanical properties of spruce wood cell walls by nanoindentation. Appl Phys A 2004;79:2069–73.

[68] Bourmaud A, Baley C. Nanoindentation contribution to mechanical characterization of vegetal fibers. Compos Part B Eng 2012;43:2861–6. doi:http://dx.doi.org/10.1016/j.compositesb.2012.04.050.

[69] Huang Y, Fei B, Wei P, Zhao C. Mechanical properties of bamboo fiber cell walls during the culm development by nanoindentation. Ind Crops Prod 2016;92:102–8.

[70] Gindl W, Schoberl T, Schöberl T. The significance of the elastic modulus of wood cell walls obtained from nanoindentation measurements. Compos Part A Appl Sci Manuf 2004;35:1345–9.

[71] Tze WTY, Wang S, Rials TG, Pharr GM, Kelley SS. Nanoindentation of wood cell walls: Continuous stiffness and hardness measurements. Compos Part A Appl Sci Manuf 2007;In Press,:945–53.

[72] Wimmer R, Lucas B. Comparing mechanical properties of secondary and cell corner middle lamella in spruce wood. IAWA J 1997;18:77–88.

[73] Doumbia ASAS, Castro M, Jouannet D, Kervoëlen A, Falher T, Cauret L, et al. Flax/polypropylene composites for lightened structures: Multiscale analysis of process and fibre parameters. Mater Des 2015;87:331–41. doi:10.1016/j.matdes.2015.07.139.

[74] Arnould O, Siniscalco D, Bourmaud A, Le Duigou A, Baley C. Better insight into the nano-mechanical properties of flax fibre cell walls. Ind Crops Prod 2017;97:224–8. doi:10.1016/j.indcrop.2016.12.020.

FIGURES

Figure 2. XRD spectra of date palm tree stem fibres. Error bars indicate 1 std. dev.

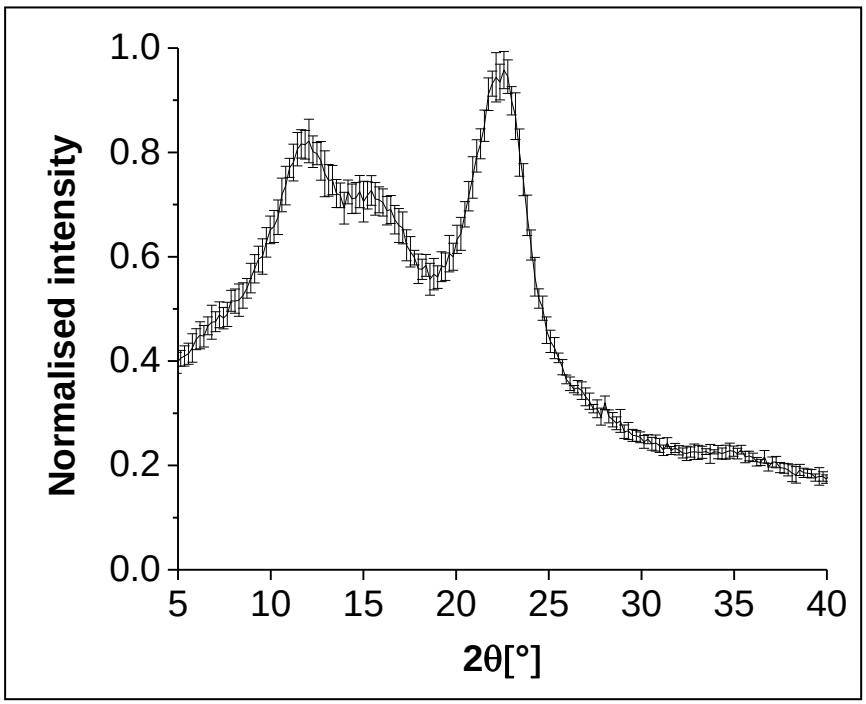

Figure 2. Fibre cross-section shape (bold black line) and area (shaded region) was estimated using a Fibre Dimensional Analysis System (FDAS). The coloured lines show the lines of path of laser beams that were tangential to a fibre surface.

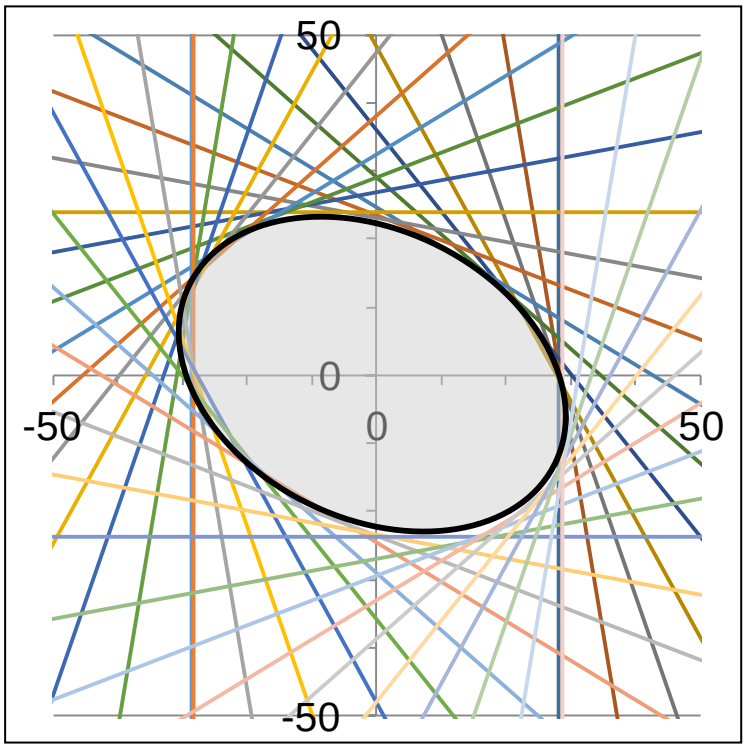

Figure 3. Schematic view of fibre bundles origin and identification.

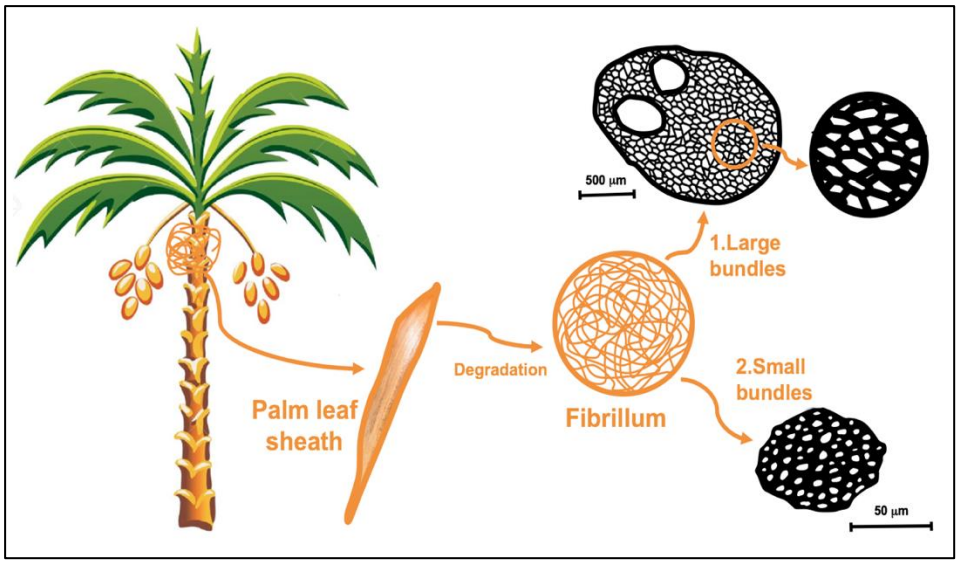

Figure 4. Optical microscope observations, scale bars are 100µm in all the micrographs.

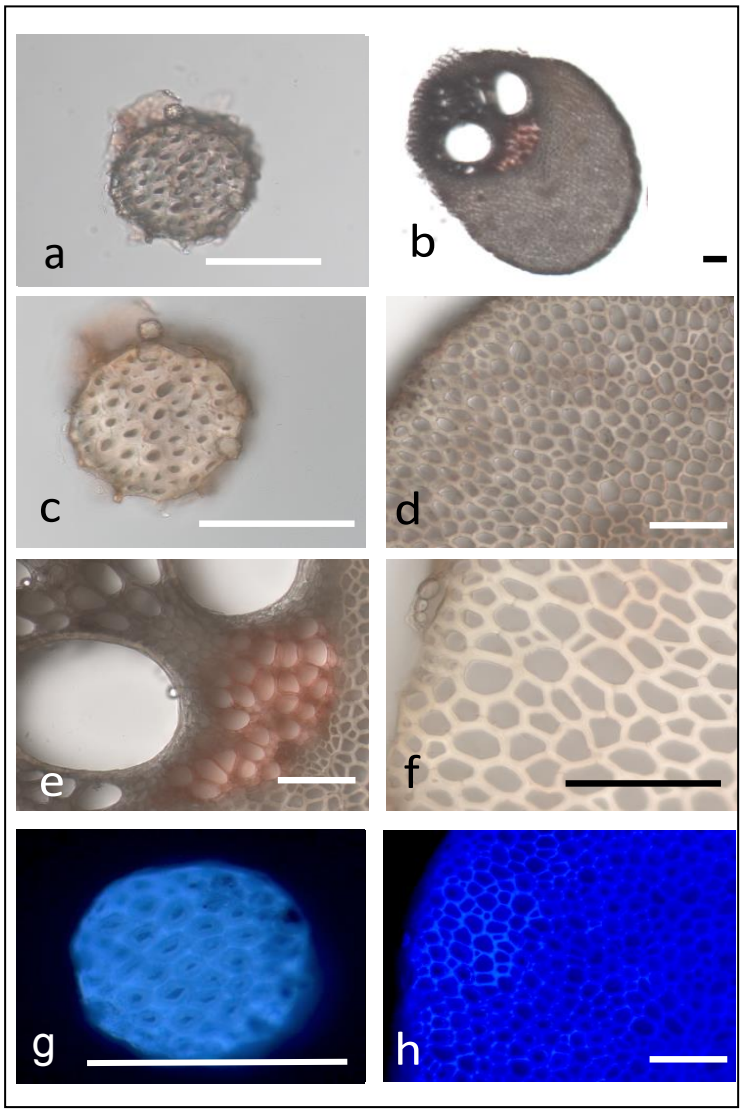

Figure 5. SEM observations of silica bodies.

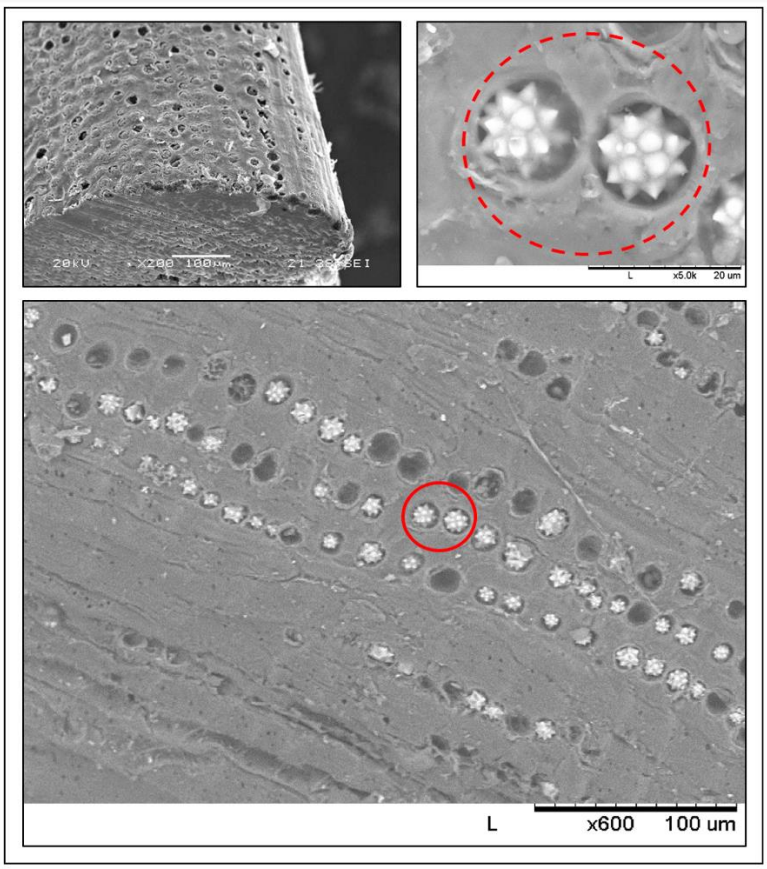
20kV
L
x5.0k
20 um
L
x600
100 um

Figure 6. Thermal degradation behaviour of date palm fibres in comparison to other natural fibres.

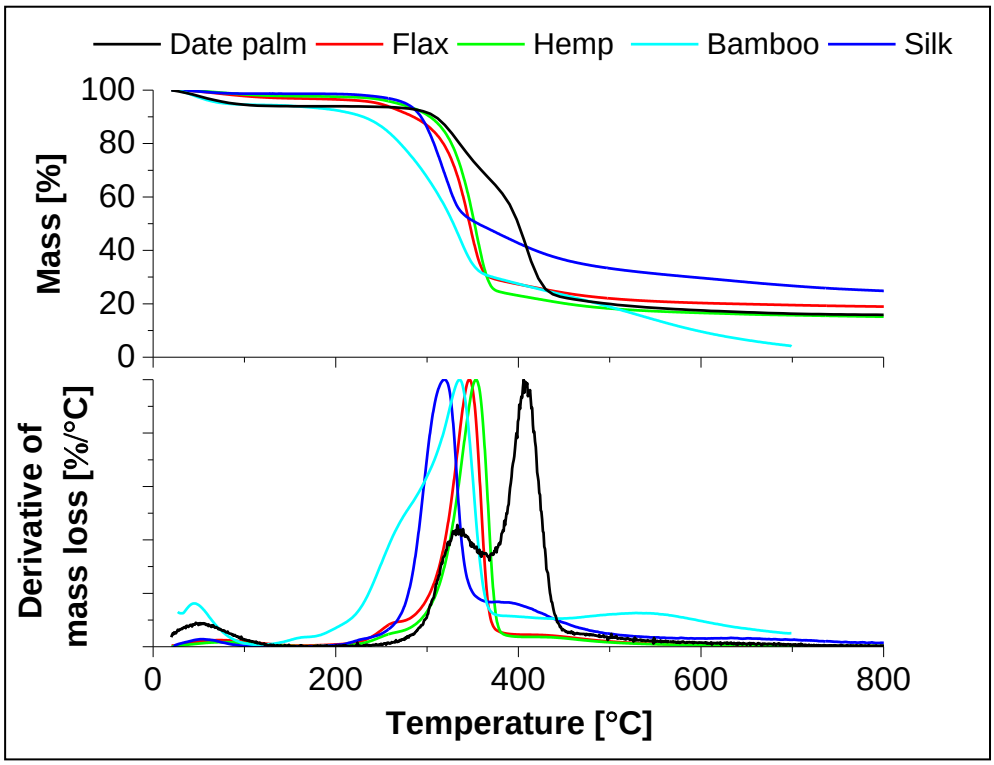

Figure 7. Moisture sorption behaviour of date palm tree stem fibres in comparison to other natural fibres. Data on other natural fibres from Hill et al [57].

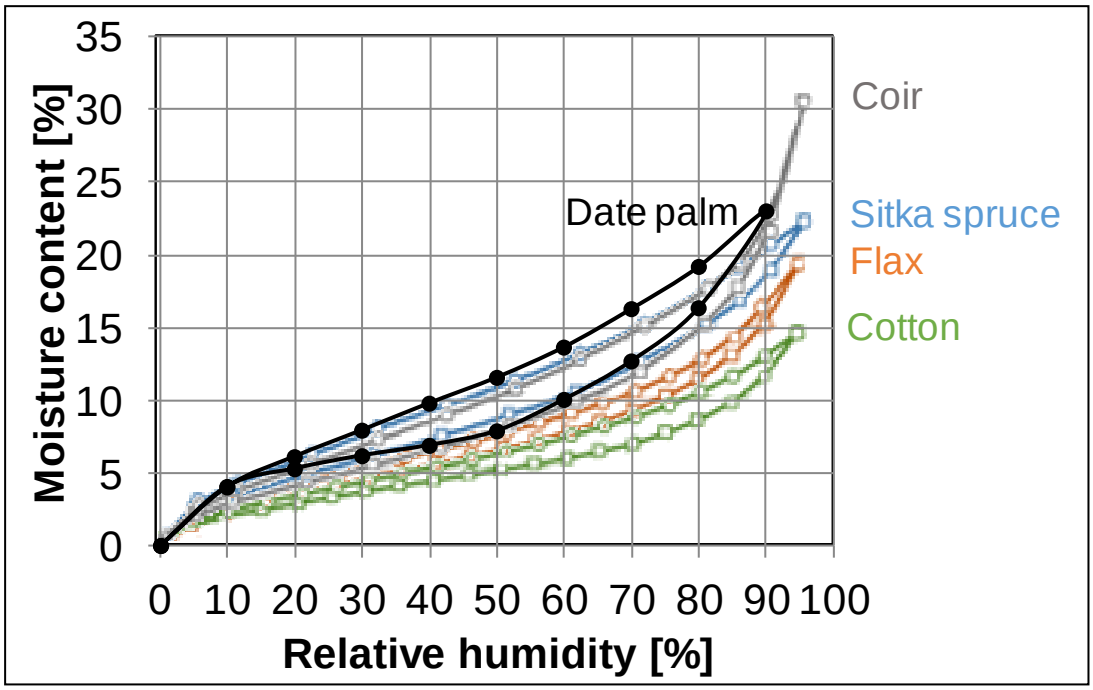

Figure 8. Materials Ashby chart of absolute (a) and specific (b) tensile stiffness and strength. Adapted from [2].

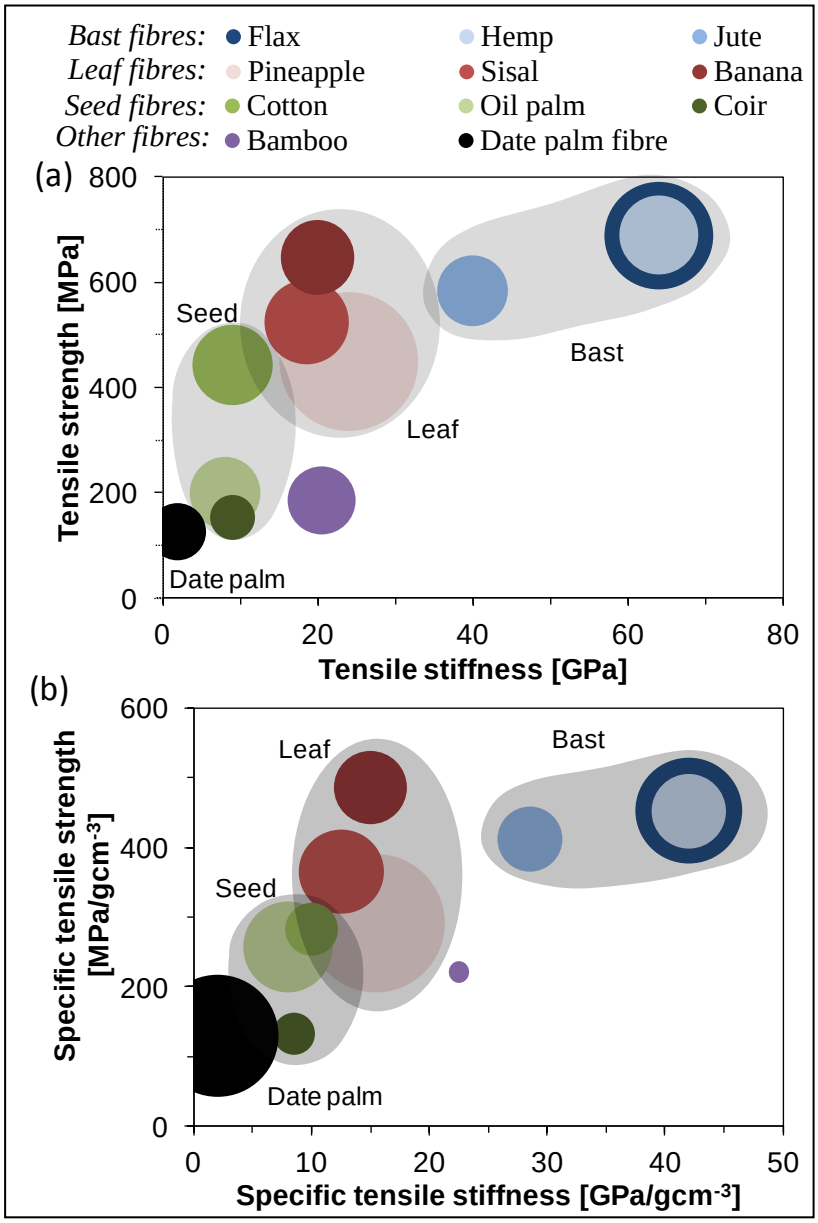

Figure 9. PF-QNM modulus mapping obtained for large and small palm bundles. A profile of the stiffness is indicated under each image, corresponding to the black line.

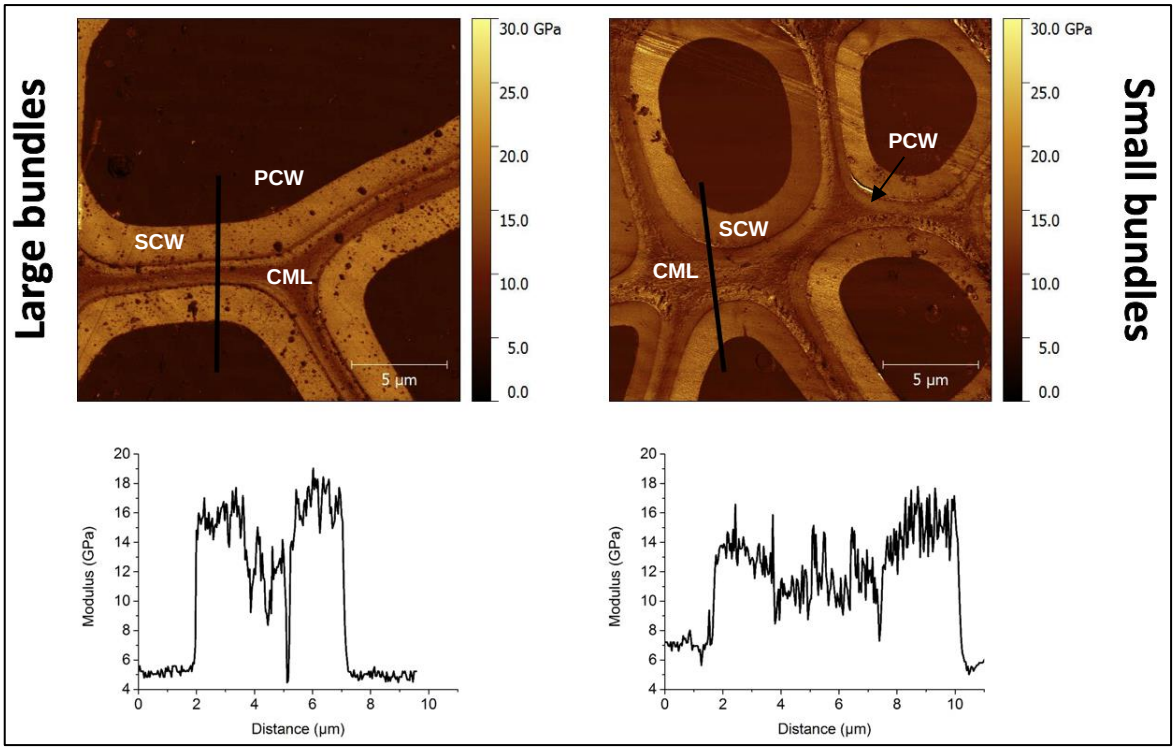

TABLES

Table 1. Chemical composition (dry wt%; mean ± st. dev.) of the date palm tree fibres.

Carbohydrate analysis (our study)									
Fuc	**Ara**	**Rha**	**Gal**	**Glc**	**Xyl**	**Man**	**GalA**	**GlcA**	**Total**
0.09 ±0.01	1.34 ±0.07	0.27 ±0.01	0.78 ±0.03	45.08 ±3.40	23.22 ±0.89	0.21 ±0.01	1.38 ±0.18	0.43 ±0.28	72.80 ±4.88

	Cellulose	**Hemicellulose**	**Lignin**	**Ash**	**Other**	**Reference**
Leaf sheath fibre	45.1±3.4	27.7±1.5	16.9±0.3	1.7±0.1	8.6	This study
Literature data – Palm elements						
Palm fibrillum	50.6±1.3	8.1±0.3	31.9±1.3	6.8±0.2	6.6	[44]
Palm leaf sheath	34.0±0.7	28.9±1.8	18.2±0.7	12.3±0.2	2.5	[44]
Palm leaflets	29.7±1.3	23.3±1.2	11.6±1.3	9.2±0.4	16.5	[44]
Palm rachis	39.8±0.9	31.4±3.2	14.0±0.9	9.2±0.1	2.5	[44]
Palm leaf sheath	28.2	20.6	44.1	-	-	[45]
Literature data – Other plant fibres						
Abaca	60.8-68.0	17.5-21	5-15.1	-	-	[46,47]
Bamboo	36.1-54.6	11.4-16.6	20.5-28.5	-	-	
Coir	32.0-43.4	3.3	40-45.8	-	-	
Flax	60-85	15.8-35.6	1-3	-	-	
Hemp	55-90	15	2-5	-	-	
Jute	58.0-71.5	15.6-26.0	11.8-16	-	-	
Kenaf	52.0-61.2	18.5-29.7	12.9-16.1	-	-	
Sisal	52.8-65	19.3	11.1-13.5	-	-	

Table 2. Comparison of mechanical and governing bio-chemical properties of our date palm tree stem fibres with various other plant fibres. Data from [47] and references therein.

	Fibre	Tensile modulus [GPa]	Tensile strength [MPa]	Failure strain [%]	Cellulose content [dry wt%]	Cellulose crystallinity [%]	Microfibril angle, MFA [°]
	Date palm leaf sheath (our study)	1.8±0.6	131±34	20.9±7.6	45±3	41±3	26.1±14.2
	Date palm (other studies)	0.3-7.5	58-203	5-50	35-50	30-40	25-30
Bast	Flax	28-100	343-1035	2.7-3.2	64-71	70-90	5-10
Bast	Hemp	32-60	310-900	1.3-2.1	70-74	70-90	2-6
Bast	Jute	25-55	393-773	1.4-3.1	61-72	60-80	8
Leaf	Sisal	9-28	347-700	2.0-2.9	66-78	50-70	10-25
Leaf	Pineapple	6-42	170-727	0.8-1.6	70-82	44-60	10-15
Leaf	Banana	8-32	503-790	3.0-10.0	44-64	45-55	10-12
Seed	Cotton	5-13	287-597	6.0-8.0	85-93	40-50	46
Seed	Coir (coconut palm)	4-6	131-175	15.0-30.0	32-43	27-33	30-49
Seed	Oil palm	3-4	248	25.0	40-50	20-30	42-46
	Bamboo	11-30	140-230	1.3	26-60	40-60	8-11

Table 3. Palm bundles nanoindentation properties.

	Number of measurements	Nanoindentation modulus (GPa)	Nanoindentation hardness (MPa)
Large bundles	32	14.3±1.8	469±93
Small bundles	29	15.8±2.4	531±77